Journal of Civil Engineering and Materials Application
Journal home page: http://journals.lexispublisher.com/jcema

Received: 22 March 2017 • Accepted: 28 June 2017

Research

doi: 10.15412/J.JCEMA.12010105

# Numerical Simulation of Turbulence and Flow Velocity Distribution Around the Spur Dike Using FLUENT

Sayed Hamid Reza Barnjani[1*], Ahmad Safari[2], Behrooz Moradi Mofrad[2]

[1] Department of Civil Engineering, Bushehr Unit, Islamic Azad University, Bushehr, Iran

[2] Department of Civil Engineering, Yasuj Branch, Yasouj University, Kohgiluyeh and Boyer Ahmad, Iran

*Correspondence should be addressed to Sayed Hamid Reza Barnjani, Department of Civil Engineering, Bushehr Unit, Islamic Azad University, Bushehr, Iran; Tell: +989368835979; Fax: +987432228450; Email: hhaammiidd.0917@gmail.com.

## ABSTRACT

Spur dikes are the intersecting or transverse structures, which are projected from the river bank toward the flow axis and cause diversion and direction of the flow from the banks towards central axis of the river. This structure affects the flow lines and causes change in the river flow pattern and protects the banks against erosion. Recognition of the flow pattern around a spur dike could help in a better understanding of the scour pattern and, as a result, achieving an accurate value of maximum scour depth. In this study, the k-$\varepsilon$ turbulence models are investigated in determining the rotational flow and flow field around the spur-dike using FLUENT software. The results show that the software incorporating the k-$\varepsilon$ model could appropriately model velocity distribution around the spur dike and the results exhibit a good compatibility with an average error of 9.24%.

**Key words: Spur dike, Flow pattern, Velocity distribution, Turbulence model.**


*Journal of Civil Engineering and Materials Application is* published by *Lexis Publisher*; Journal p-ISSN xxxx-xxxx; Journal e-ISSN 2588-2880.

## 1. INTRODUCTION

One of the indirect and common methods in control of erosion and protection of river banks is the use of spur dike (1). Spur dikes are the intersecting or transverse structures which are projected from the river bank toward the flow axis and cause diversion and direction of the flow from the banks towards central axis of the river (2). This structure affects the flow lines, causes change in the river flow pattern and protects the banks against erosion. Recognition of the flow pattern around a spur dike could help in better understanding of the scour pattern and, as a result, achieving an accurate value of maximum scour depth (3). In this respect many research works have been conducted by various researchers. Ishi et al. (1983), performed studies on the effect of some non-dimensional parameters on the separation zone geometry at downstream of the spur dike and stated that the Froude number has impact on the geometry of the separation zone and for a spur dike with a length equal to 10% of the canal width, the length of this zone is 0-12 times the spur dike length and its width is maximum two times the spur dike length from the bank. By increase in the spur dike length from 10% of the canal width to 40% of it, the length of separation zone increases from 7 to 12 times the length (4). Chen and Ikeda (1997) performed relatively comprehensive research on the flow pattern around a single spur dike in the straight alignment. In this research the formation, development and transfer of horizontal eddies around the spur dike tip are experimentally studied. The abovementioned researchers found that transient eddies were separated from the spur dike tip and transferred downstream in an alternative way. Analyzing the obtained results, they found that the mean migration velocity of eddies was nearly constant and a bit higher than 1.5% of the mean velocity (5). Kadota et al. (2006) investigated flow structure around a single spur dike in two submerged and semi-submerged states and for the shallow depth flow condition. Kadota et al. used the surface particle tracking technique and measured the flow pattern in a wide area around the single spur-dike with sloped sides. The spur-dike was modeled after the constructed

spur dikes in Hiji River in Japan. Based on the presented results by the above researchers for non-submerged spur dike, the energy contained vortices were formed along the shear layer and extended downstream. In the non-submerged spur dike, the alignment of energy contained vortices diverted toward the canal bank and, unlike the submerged spur dike, they were formed in a relatively distant location from the spur dike body (6). Asadzadeh (2012) experimentally investigated the flow field around a single spur dike with sloped sides. The obtained results showed that at the back of the spur dike, with reduced flow velocity, a stagnation zone is formed and the flow velocity is increased in the middle areas. Therefore a portion of the flow moves upward and a portion moves downward where the pressure is lower. The downstream flow causes formation of horseshoe vortices. Two intense velocity zones were formed, where the first one corresponded to the intense velocity at the main core of flow caused by reduced flow width, and the other intense velocity zone was associated with the local intense velocity downstream the spur dike and out of the shear layer (7). Salajegheh (2003), studying the flow pattern around the spur-dike, concluded that with a series of two spur dikes located in the bend, by increase in the flow depth, the distance of the center of vortices to the first spur dike is reduced (8). Molinas et al. (1998) experimentally investigated the shear stress distribution around the bridge abutment which has a behavior similar to that of a spur dike. In this research effects of the flow Froude number and contraction ratio (ratio of the reduced width to total canal width) on the maximum shear stress value at the abutment tip and also the overall shear stress distribution were investigated. The performed studies show that, depending on the amount of abutment projection and flow condition, the shear stress was intensified around the abutment and the deep flow velocities at upstream abutment were increased about 50% with respect to the upstream flow velocity (9). Kuhnle et al. (2002, 2008), experimentally and numerically (using CCHE3D) investigated the flow pattern around a submerged trapezoidal shaped spur dike with a straight alignment for two cases of the flat bed and scoured (balanced) bed. The results showed that the length of vortex zone from the flow separation point to the reattachment point was 1.6 L. The performed numerical simulation had acceptable results except for the recirculation zone downstream of the spur dike and the maximum shear stress occurred downstream of the spur dike and was 2.7 times the shear stress upstream of the spur-dike (10, 11). Vaghefi et al. (2016) numerically investigated the effect of submergence on the flow pattern around a T-shaped spur dike located in the 90° bend. For this purpose, they used FLOW3D software and, for verification, they used the experimental studies in the non-submerged state. The results showed that increase in the dimensions and number of vortices was associated with the submergence percentage. Also the length and width of the separation zone in this case were 1.6 times and 1.5 times the corresponding length and width of the separation zone in the case of non-submergence (12). According to the abovementioned studies and as the experimental studies are time and cost consuming, the necessity of numerical studies and investigating the numerical methods in determining flow field around a spur dike becomes evident. On the other hand, due to the turbulent nature of flow around a spur dike, in this study the K-$\varepsilon$ turbulence model is utilized in determining the rotational flow and flow field around the spur dike.

## 2. NUMERICAL MODELING

In this paper, FLUENT software is used to investigate the flow pattern around the spur dike. FLUENT is a powerful software which analyses both the fluid flow and heat transfer problems and has a high capability in solving disorganized grids with complex geometries. Among the unique features of this software is the vast materials data base, high flexibility in dealing with user defined functions (UDF), ability to modify the grid during analysis based on the variation in the solution parameters, taking advantage of a variety of discretization techniques, taking advantage of various turbulence models including k-$\varepsilon$, k-$\omega$, RSM, Spalart-Allmaras, DES, LES and their derivatives, and having a wide variety of boundary conditions (13). FLUENT uses unstructured grids to reduce the time of flow-field solution and it also simplifies geometric modeling and mesh generation stages thus more complex grids could be modeled. It should be noted that it is better to prepare the geometry and initial mesh outside of FLUENT environment using such software as Gambit (14).

## 3. GOVERNING EQUATIONS

For modeling of this problem the finite volume method is used, and, to account for the flow turbulence affects, the k-$\varepsilon$ model is incorporated. The governing laws of an incompressible viscous fluid flow are stated by the continuity equation and three momentum equations along the three coordinate axes which are known as Navier-Stokes equations. These equations in fact state the consistency of mass and momentum in mathematical language. The continuity equation or the conservation of mass equation in a fluid flow is stated as equation (1) (15):

$$\frac{\partial \rho}{\partial t} + \frac{\partial}{\partial x_i}(\rho u_i) = 0 \quad (1)$$

Navier-Stokes equations, are the governing momentum equations for viscous Newtonian fluids flow and the tensor form of these equations is stated in the Cartesian coordinates as equation (2):

$$\rho\left(\frac{\partial u_i}{\partial t} + u_j\frac{\partial u_i}{\partial x_j}\right) = -\frac{\partial P}{\partial x_i} + \frac{\partial \tau_{ij}}{\partial x_j} + \rho g_i \quad (2)$$

The left hand side of the above equation states the fluid acceleration which includes the temporal and spatial changes of the velocity and the terms at the right hand side state the force per unit mass. The standard k-$\varepsilon$ model is a semi-empirical model based on model transport equations for the turbulent kinetic energy (k) and its dissipation rate ( $\varepsilon$). The model transport equation for k is derived from the exact equation, while the models transport equation for $\varepsilon$ is obtained using physical reasoning. In derivation of k-$\varepsilon$ model it is assumed that the flow is fully turbulent and effects of molecular viscosity are negligible. The turbulent kinetic energy, k, and its rate of dissipation,$\varepsilon$ are obtained from the following transport equations (3) and (4):

$$\frac{\partial(\rho K)}{\partial t}+\frac{\partial(\rho K u_i)}{\partial x_i}=\frac{\partial}{\partial x_j}\left[\left(\mu+\frac{\mu_t}{\sigma_k}\right)\frac{\partial K}{\partial x_j}\right]+G-\rho\varepsilon \quad (3)$$

$$\frac{\partial(\rho\varepsilon)}{\partial t}+\frac{\partial(\rho\varepsilon u_i)}{\partial x_i}=\frac{\partial}{\partial x_j}\left[\left(\mu+\frac{\mu_t}{\sigma_\varepsilon}\right)\frac{\partial\varepsilon}{\partial x_j}\right]+C_{1\varepsilon}\frac{\varepsilon}{K}G-C_{2\varepsilon}{}^{*}\rho\frac{\varepsilon^2}{K}G \quad (4)$$

In the above equations:

$$C_{2\varepsilon}{}^{*}=C_{2\varepsilon}+\frac{C_\mu\eta^3(1-\eta/\eta_0)}{1+\beta\eta^3}$$

$$\eta=\frac{SK}{\varepsilon}$$

$S=(2S_{ij}S_{ij})^{0.5}$ And

$$S_{ij}=\frac{1}{2}(u_{ij}+u_{ji})$$

Where $\mu_t$, is the turbulent viscosity which is calculated by equation (5) using k (turbulent kinetic energy) and $\varepsilon$ (its rate of dissipation):

$$\mu_t=\rho C_\mu\frac{K^2}{\varepsilon} \quad (5)$$

Turbulent kinetic energy, G and consequently the mean velocity gradient are defined according to equation (6):

$$G=\mu_t\left(\frac{\partial u_i}{\partial x_j}+\frac{\partial u_j}{\partial x_i}\right)\frac{\partial u_i}{\partial x_j} \quad (6)$$

## 4. MODEL PREPARATION

For verification the Asadzadeh research was incorporated which was performed experimentally (7). This spur dike has a sloped wall of 75 degrees and the crest length of 10 cm and the crest width of 5cm, also its height from the bed is 25cm. The flow velocity is 0.3 m/s and the flow depth is 11cm. The canal length is 6m and its width is 45cm and the location of spur dike crest center is 2.5cm from the upstream. The spur dike characteristics are given in Table 1.

**Table 1. Spur-dike and flow characteristics in the experimental study**

| Mean velocity m/s | flow depth cm | spur-dike length cm | spur-dike angle with respect to flow direction | spur-dike side slope | spur-dike tip slope |
|---|---|---|---|---|---|
| 0.3 | 11 | 10 | 90 | 75 | 90 |

To generate the initial geometry, Gambit software is incorporated, and a sample of meshing and program environment is shown in Figure 1. As seen in the figure, due to intense variations in velocity in the vicinity of spur dikes, a denser mesh is used here with respect to other points. The mesh size was obtained after a number of trials and errors and totally 211952 elements were used for the entire geometry. In this program, the boundary conditions are used for input, output and wall at different sections. As variation in the water surface was negligible in this problem, we have ignored the two-phase flow model and taking into account the water surface profile (16).

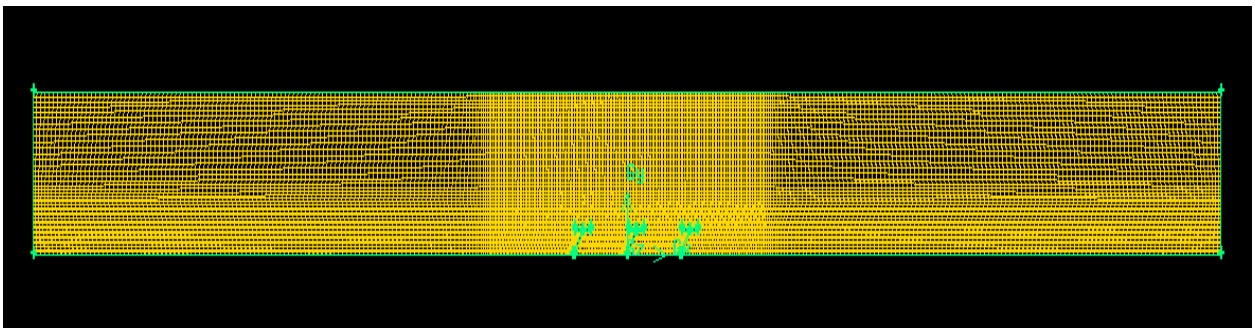

**Figure 1. Meshing of the flow field meshing sing Gambit software**

## 5. RESULTS AND DISCUSSION

The model validation results in determining the longitudinal and transverse components of velocity around the spur dike and at 2 cm level from the bed are shown in

Figure 2 -a to 2-d. These figures include both the experimental study by Asadzadeh and the present research. According to the experimental and numerical results, it is observed that the flow structure is changed when it reaches the spur-dike. Regarding fig.2, by moving toward the spur dike, the flow is affected by it and due to contraction in the section, the longitudinal flow velocity is greatly increased. Also, at the back of the spur dike, due to the presence of negative longitudinal flow velocity, the rotational flow is formed. Maximum transverse velocity occurs at the upstream edge of the spur dike which is due to intense flow diversion with respect to the upstream edge.

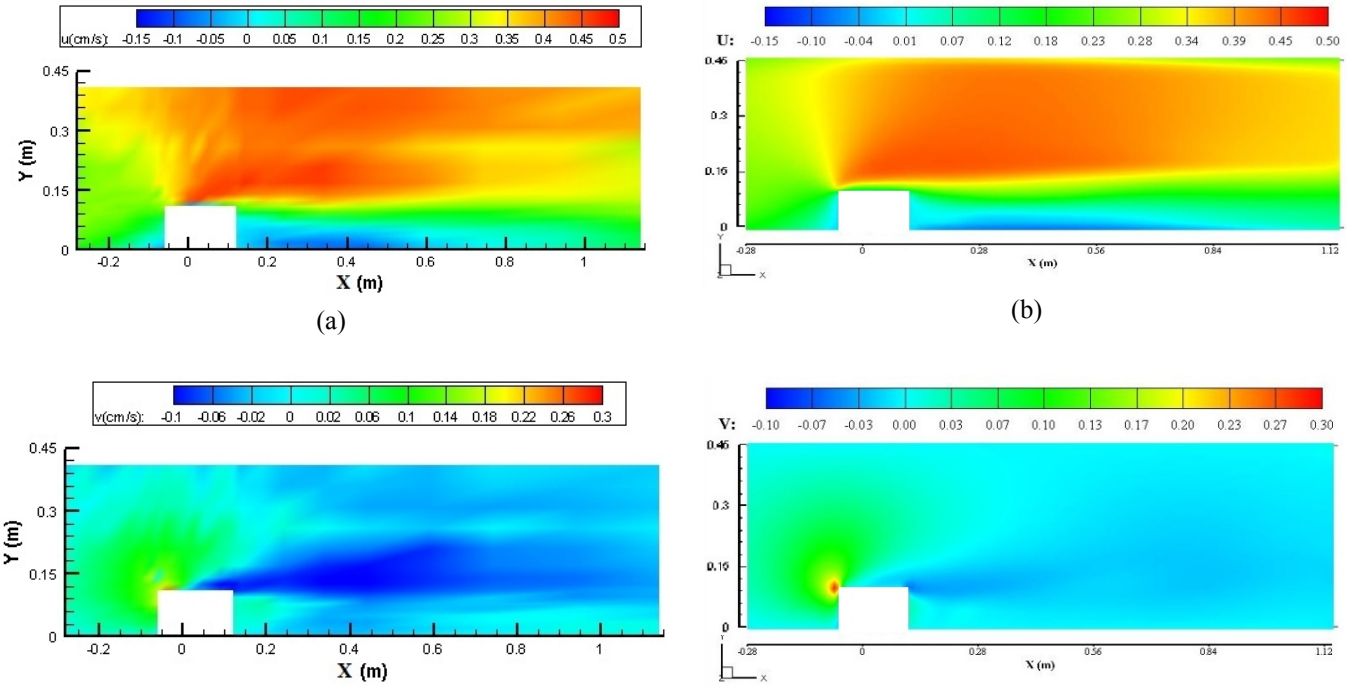


**Figure 2. Velocity distribution around the spur dike, a) longitudinal velocity distribution in the experimental study, b) longitudinal velocity distribution in the present study (k-$\varepsilon$ model), c) transverse velocity distribution in the experimental study, d) transverse velocity distribution in the present study (k-$\varepsilon$ model)**

According to Figure 3, the k-$\varepsilon$ model yields more logical responses with respect to those of LES model in terms of quality, but quantitative validation seems to be essential. Thus variations in the longitudinal and transverse velocities at the center line of canal were extracted from the software and were compared to those velocities in the experimental model.

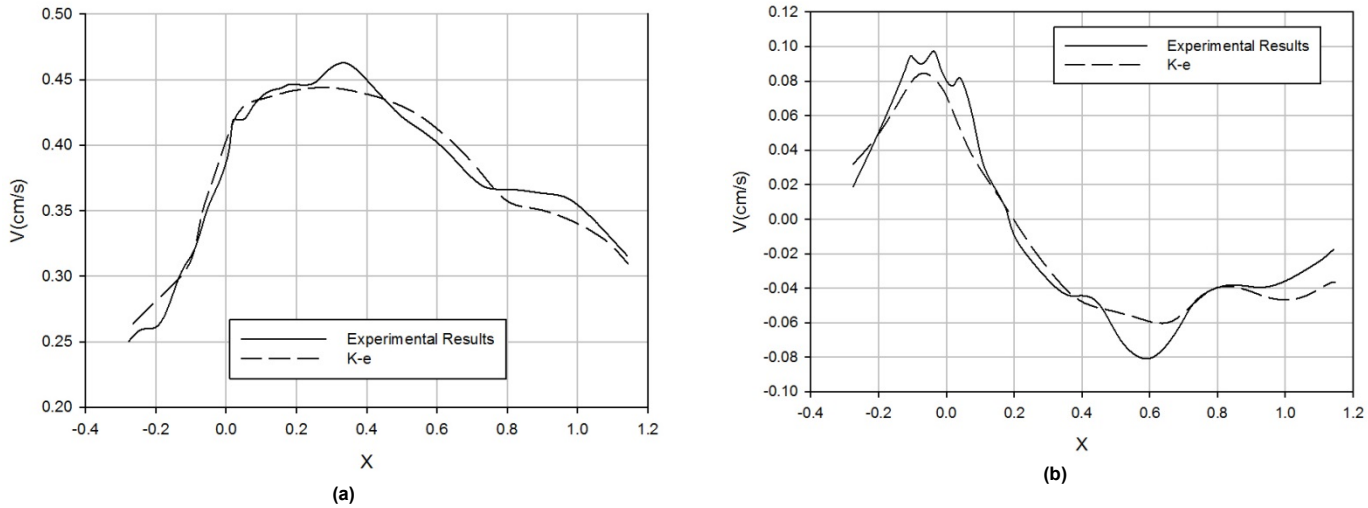


**Figure 3. Comparison between the velocities at the center line of flow at 2cm height from the bed in the experimental and numerical models; a) variation in the longitudinal velocity, b) variation in the transverse velocity**

For quantitative investigation and comparison between the experimental results and the present model, the error values are calculated from the following expression (17):

$$\text{Error} = \frac{1}{N}\sum_{i=1}^{N}\frac{\varphi_i - \varphi_i'}{\varphi_i'} \times 100 \quad (7)$$

Where N is the number of data, $\varphi_i$ is the value of obtained quantity by the present model and $\varphi_i'$ is the value of obtained quantity from the experimental study. Using the experimental data and the numerical model results given in Fig.3, the corresponding error for longitudinal velocity component is 7.46% and that of transverse velocity component is 11.02%. Therefore the presented model has an average error equal to 9.24% which is in the acceptable range.

## 6. CONCLUSION

In the present study, the flow pattern around the spur dike was investigated using FLUENT software and k-$\varepsilon$ turbulence model. In addition, a comparison was made between the present model results and those of the experimental study. The results show that the flow structure changes when it approaches the spur dike. By moving toward the spur dike, the flow is affected by the spur dike and, due to contraction of the section, the longitudinal flow velocity is increased. Also at the back of the spur dike, due to the presence of negative longitudinal velocity, rotational flow is formed. The maximum transverse velocity occurs at the upstream edge of the spur dike, which is due to intense flow diversion from the upstream edge. The obtained results from the numerical modeling using FLUENT software and comparing them with those of the experimental study reveals that the software well simulated the flow pattern around the spur dike and an average error of 9.24% between the simulation results and those of the experimental study is acceptable.

## FUNDING/SUPPORT

Not mentioned any Funding/Support by authors.

## ACKNOWLEDGMENT

Not mentioned any acknowledgment by authors.

## AUTHORS CONTRIBUTION

This work was carried out in collaboration among all authors.

## CONFLICT OF INTEREST

The author (s) declared no potential conflicts of interests with respect to the authorship and/or publication of this paper.

## REFERENCES

1. Osman AM, Thorne CR. Riverbank stability analysis. I: Theory. Journal of Hydraulic Engineering. 1988;114(2):134-50.
2. Lagasse PF. Riprap design criteria, recommended specifications, and quality control: Transportation Research Board; 2006.
3. Vaghefi M, Ghodsian M, Salehi Neyshaboori S. Experimental study on the effect of a T-shaped spur dike length on scour in a 90 channel bend. Arabian Journal for Science and Engineering. 2009;34(2):337.
4. Ishii C, Asada H, Kishi T, editors. Shape of separation region formed behind a groyne of non-overflow type in rivers. XX IAHR Congress, Moscow, USSR; 1983.
5. Kadota A, Suzuki K, Uijttewaal W, editors. The shallow flow around a single groyne under submerged and emerged conditions. River Flow; 2006.
6. Fei-Yong C, Ikeda S. Horizontal separation flows in shallow open channels with spur dikes. Journal of Hydroscience and hydraulic Engineering. 1997;15(2):15-30.
7. Ghodsian M, Vaghefi M. Experimental study on scour and flow field in a scour hole around a T-shape spur dike in a 90 bend. International Journal of Sediment Research. 2009;24(2):145-58.
8. Safarzadeh A, Salehi Neyshabouri SAA, Zarrati AR. Experimental investigation on 3D turbulent Flow around straight and T-Shaped groynes in a flat bed channel. Journal of Hydraulic Engineering. 2016;142(8):04016021.
9. Molinas A, Kheireldin K, Wu B. Shear stress around vertical wall abutments. Journal of Hydraulic Engineering. 1998;124(8):822-30.
10. Kuhnle RA, Jia Y, Alonso CV. Measured and simulated flow near a submerged spur dike. Journal of Hydraulic Engineering. 2008;134(7):916-24.
11. Kuhnle RA, Alonso CV, Shields Jr FD. Local scour associated with angled spur dikes. Journal of Hydraulic Engineering. 2002;128(12):1087-93.
12. Vaghefi M, Safarpoor Y, Hashemi SS. Effects of relative curvature on the scour pattern in a 90° bend with a T-shaped spur dike using a numerical method. International Journal of River Basin Management. 2015;13(4):501-14.
13. Yazdi J, Sarkardeh H, Azamathulla HM, Ghani AA. 3D simulation of flow around a single spur dike with free-surface flow. Intl J River Basin Management. 2010;8(1):55-62.
14. Salaheldin TM, Imran J, Chaudhry MH. Numerical modeling of three-dimensional flow field around circular piers. Journal of Hydraulic Engineering. 2004;130(2):91-100.
15. Vaghefi M, Shakerdargah M, Fiouz A, Akbari M. Numerical Investigation of the Effect of Froude Number on Flow Pattern around a Single T-shaped Spur Dike in a Bend Channel. International Journal of Engineering Research. 2014;3(5):351-5.
16. Hirt CW, Nichols BD. Volume of fluid (VOF) method for the dynamics of free boundaries. Journal of computational physics. 1981;39(1):201-25.
17. Karami H, Basser H, Ardeshir A, Hosseini SH. Verification of numerical study of scour around spur dikes using experimental data. Water and environment journal. 2014;28(1):124-34.